JOURNAL OF MAGNETIC RESONANCE **126,** 221–228 (1997)
ARTICLE NO. MN971165

Optimization of Adiabatic Selective Pulses

Daniel Rosenfeld,*,† Shimon L. Panfil,‡ and Yuval Zur‡

*School of Physics and Astronomy, Tel-Aviv University, Tel-Aviv 69978, Israel; and ‡Elscint MRI Center, P.O. Box 550, Haifa 31004, Israel

Received November 12, 1996; revised March 11, 1997

Adiabatic RF pulses play an important role in spin inversion due to their robust behavior in presence of inhomogeneous RF fields. These pulses are characterized by the trajectory swept by the tip of the B_{eff} vector and the rate of motion upon it. In this paper, a method is described for optimizing adiabatic inversion pulses to achieve a frequency-selective magnetization inversion over a given bandwidth in a shorter time and to improve slice profile. An efficient adiabatic pulse is used as an initial condition. This pulse allows for flexibility in choosing its parameters; in particular, the transition sharpness may be traded off against the inverted bandwidth. The considerations for selecting the parameters of the pulse according to the requirements of the design are discussed. The optimization process then improves the slice profile by optimizing the rate of motion along the trajectory of the pulse while preserving the trajectory itself. The adiabatic behavior of the optimized pulses is fully preserved over a twofold range of variation in the RF amplitude which is sufficient for imaging applications in commercial high-field MRI machines. Design examples demonstrate the superiority of the optimized pulses over the conventional sech/tanh pulse. © 1997 Academic Press

Adiabatic fast passage has long been used to invert a selected band of spins. These pulses retain their robustness even when subjected to nonuniform RF amplitude. The pulse is defined by its instantaneous amplitude $\omega_1(t) = \gamma B_1(t)$ and frequency $\omega(t)$ and is most conveniently studied in the frequency frame which is a frame of reference rotating at the instantaneous frequency of the pulse (*1*). It operates by causing the magnetization vector **m** to follow the effective field vector $\boldsymbol{\omega}_{\text{eff}} = \gamma \mathbf{B}_{\text{eff}}$ which is composed of the RF field ω_1 and the resonance offset $\Delta\omega(\omega_0, t) = \omega(t) - \omega_0$, ω_0 being the Larmor frequency of the spin we are inspecting. The adiabatic theorem (*2*) asserts that the magnetization vector **m** remains spin-locked to $\boldsymbol{\omega}_{\text{eff}}$ provided that the rate of precession of **m** about $\boldsymbol{\omega}_{\text{eff}}$ is much faster than the angular velocity of the motion of $\boldsymbol{\omega}_{\text{eff}}$. Mathematically this is expressed by the adiabatic condition (*3*)

$$\Gamma(\omega_0, t) \gg 1, \qquad [1]$$

where Γ is the adiabatic parameter

$$\Gamma(\omega_0, t) = \frac{\|\boldsymbol{\omega}_{\text{eff}}(\omega_0, t)\|}{|\dot{\theta}(\omega_0, t)|}, \qquad [2]$$

and $\tan\theta = \Delta\omega/\omega_1$. Inversion is obtained when the effective field moves the longitudinal magnetization M_z from the $+z$ to the $-z$ axis over a wide band of Larmor frequencies.

In the frame of reference of the slice center, i.e., for $\boldsymbol{\omega}_0 = \omega_c$, we may plot the route traced by the tip of the ω_{eff} vector. This graph of $\omega_1(t)$ vs $\Delta\omega(\omega_c, t)$ is called the trajectory of the adiabatic pulse. An adiabatic pulse is characterized by its trajectory and the rate of motion of $\boldsymbol{\omega}_{\text{eff}}$ upon it. Three classic examples (expressed here as amplitude/frequency modulation functions) include the sech/tanh (*4*), sin/cos (*5*), and const/tan (*3*). Several methods have been proposed for the optimization of the modulation functions in adiabatic pulses. Some were derived from the adiabatic criterion, such as NOM (*6*) and its derivatives (*7–12*); other methods employ optimal control theory (*13–15*).

In our previous work, Ref. (*16*), we presented a new adiabatic inversion pulse for which the designer is able to obtain a very efficient pulse when given a required set of pulse parameters. The trajectory traced by the $\boldsymbol{\omega}_{\text{eff}}$ vector has a square-like shape with rounded corners and is divided into several sections. The reader is referred to Eqs. [8] through [25] and Fig. 3 of that reference for a summary of the pulse-modulation functions and the trajectory. The pulse parameters used for the design process include the inverted bandwidth SW, the peak RF amplitude $\gamma B_{1\,\max}$ [which is designated in Ref. (*16*) and below as x_f], a parameter c_0 associated with the transition width, and $\bar{\gamma}_0$[1] which is related to the adiabaticity of the pulse and determines its total duration. Note that the first three parameters are defined in units of angular frequency and the fourth is unitless. The parameter $\bar{\gamma}_0$ represents the minimal value attained by the adiabatic parameter Γ along each segment of the pulse. This can be demonstrated as follows: take any point along the trajectory

† To whom correspondence should be addressed. Present address: Elscint MRI Center, POB 550, Haifa 31004, Israel

[1] In this paper, we use $\bar{\gamma}_0$, a unitless parameter related to γ_0 in Ref. (*16*) by $\bar{\gamma}_0 = 2\pi\gamma_0$.

1090-7807/97 $25.00

of the pulse, say at time instance t_0, and compute the value of $\Gamma(\omega_0, t_0)$ for this point with respect to all Larmor frequencies ω_0 in the in-slice and out-of-slice regions (*16*) where the adiabatic condition is required to be fulfilled. The pulse is designed so that the minimal value obtained is exactly $\bar{\gamma}_0$. In practice, we found that the minimal value of $\bar{\gamma}_0 \approx 4$ can still render satisfactory inversion. The parameter c_0 is related to the transition width: when the minimal value of $\bar{\gamma}_0$ is selected, the transition width is approximately $2c_0$.

The total pulse duration T is determined by summing up the time spent on each segment of the pulse [cf. Ref. (*16*)] and then multiplying by 2:

$$T = \frac{\bar{\gamma}_0}{2\pi}\left[\frac{2.18}{c_0} + \frac{(\mathrm{SW}/x_f) - 0.815}{x_f}\right]. \qquad [3]$$

This equation enables us to trade off the various parameters of the pulse to meet the design requirements: it can help us determine the optimal parameters that can be achieved for a given pulse duration or, alternatively, the minimal required duration for a predetermined set of pulse parameters. Let us demonstrate this for two extreme cases: (1) We require a transition which is as narrow as possible, but care less about the inverted bandwidth. Such a pulse is useful if we want to invert selectively the magnetization of lipid spins while leaving the magnetization of water spins intact. In this case, most of the time is spent in the ''transition region'' of the pulse [section $\overline{AB}$ in Ref. (*16*): the horizontal section close to the z axis], so that the first term in [3] is dominant over the second, yielding

$$T \approx \frac{\bar{\gamma}_0}{2\pi}\cdot\frac{2.18}{c_0} \quad \Rightarrow \quad c_0 \approx \frac{\bar{\gamma}_0}{2\pi}\cdot\frac{2.18}{T}, \qquad [4]$$

where $\bar{\gamma}_0 \approx 4$, which gives us an estimate of the lowest achievable transition width.

(2) At the other extreme from the situation just described, we would like to invert the largest possible bandwidth SW in a given pulse duration T and RF amplitude x_f. To this end, we are willing to sacrifice the transition width. Here, most of the time will be spent in the vertical sections of the trajectory which requires that the first term of Eq. [3] must be minimal. This occurs when x_0 equals x_1 [see Ref. (*16*, Eq. [15])], so that $T_{\mathrm{horiz}} = 0$ and the resulting transition width is given by $c_0 = 0.522x_f$. On the other hand, $c_0 \leqslant \mathrm{SW}/2$ since it is impossible for the transition region to exceed the inverted bandwidth. Substituting the transition width back into Eq. [3] gives

$$T = \frac{\bar{\gamma}_0}{2\pi}\cdot\left[\frac{(\mathrm{SW}/x_f) + 3.36}{x_f}\right] \quad \Rightarrow$$

$$\mathrm{SW} = x_f\cdot\left(\frac{x_f}{\bar{\gamma}_0/2\pi}\,T - 3.36\right), \qquad [5]$$

which is an estimate of the largest inverted bandwidth that can be achieved for the given pulse duration T and RF amplitude x_f. Note that our choice of $c_0 = 0.522x_f$, together with the restriction $\mathrm{SW}/2 \geqslant c_0$, results in a lower bound of 1.044 for the term in parentheses in the expression for SW in Eq. [5].

The two extreme cases were distinguished by the relative magnitude of the two terms in Eq. [3]; the conditions are such that one is dominant over the other. A range of intermediate cases may also be envisaged. For example, in order to invert a wide frequency band while maintaining a sharp transition, both terms should be of similar magnitude. The two extreme cases are exemplified below.

In contrast to the pulse we have just described, the conventional sech/tanh adiabatic pulse is less flexible in its behavior. The sech/tanh pulse enables us to select the inversion bandwidth SW and the maximal RF amplitude x_f along the trajectory. However, these two parameters determine the minimal inversion time (*4*) which is the minimal duration required by the pulse to invert the magnetization. We cannot sacrifice the transition width in order to accomplish inversion, as is possible in our pulse, because the transition width of the sech/tanh pulse is exclusively determined by its duration. These points are emphasized in the examples given below. In the Appendix, the performance of the sech/tanh pulse is quantitatively compared with that of the new adiabatic pulse.

Thus far, we have assumed that the value of $\bar{\gamma}_0$—the lowest value of Γ—is kept constant throughout the entire pulse. When using a constant $\bar{\gamma}_0$, the pulse may exhibit some imperfections in the form of increased sidelobes in the out-of-slice region or a ripple within the inverted band (the in-slice region). We now show how to use the pulse as a starting point for an optimization process which adjusts the rate of motion along the given trajectory by optimizing $\bar{\gamma}_0$ as a function of t. The theoretical background of setting up an MRI pulse optimization problem can be found in Refs. (*15, 17*). Optimality is usually measured with respect to a cost functional which expresses the Euclidean distance between the target magnetization $\mathbf{m}_d(\omega_0)$ and the actual magnetization $\mathbf{m}(\omega_0, T)$

$$J_d = \sum_{\omega_0} [\mathbf{m}(\omega_0, T) - \mathbf{m}_d(\omega_0)]^2, \qquad [6]$$

where the sum is performed over a range of Larmor frequencies which includes the region of inversion. In Ref. (*17*), we described an optimization method for adiabatic pulses in which both the amplitude and the frequency-modulation functions are optimized. The adiabaticity is incorporated into the optimization problem by enhancing the cost functional given in Eq. [6] with an additional, adiabaticity-preserving term, the purpose of which is to maintain adiabaticity during the optimization process. In this paper, in contrast, this addi-

tional term is not required. Instead, the sweep rate is the function that is optimized and, as we discuss below, adiabaticity is preserved by: (i) restricting the motion to the original pulse trajectory and (ii) forcing only forward motion of the effective field vector $\boldsymbol{\omega}_{\text{eff}}$. In addition, we benefit by reducing both the complexity (i.e., no adiabatic term) and the dimensionality (i.e., only a single function is optimized rather than two) of the problem.

We begin by breaking up the RF pulse into N segments and representing it by a piecewise-constant function with the definition

$$\omega_1[n] = \omega_1(t), \quad \omega[n] = \omega(t),$$
$$\text{for } t_{n-1} < t \leq t_n, \quad n = 1, 2, \ldots, N, \qquad [7]$$

where t_n are the sampling times with $t_0 = 0$ and $t_N = T$. The sampling intervals are given by

$$\Delta t_n = t_n - t_{n-1}, \quad n = 1, 2, \ldots, N. \qquad [8]$$

We employ a notation where the discrete time index is enclosed in square brackets to distinguish it from the continuous time variable which is enclosed in parentheses. Each sampling duration Δt_n is directly proportional to $\bar{\gamma}_0$. Consequently, the rate of motion along each segment, which is embodied by $\bar{\gamma}_0$, may be adjusted by altering the sampling time Δt_n. Therefore, the optimal pulse is described by a set of N sampling intervals $\{\Delta t_n, n = 1, 2, \ldots, N\}$, the sum of which is the pulse duration $T = \sum_{n=1}^{N} \Delta t_n$. The latter restriction can then be appended to the cost functional of Eq. [6] yielding

$$J[\Delta t_1, \Delta t_2, \ldots, \Delta t_N] = J_d + \kappa \cdot \Big(\sum_{n=1}^{N} \Delta t_n - T\Big)^2, \qquad [9]$$

where κ is a positive factor which controls the relative weighting of the two terms. κ is determined experimentally: the larger the κ, the better will the total-time constraint be obeyed. This, however, will be done at the expense of the slice profile quality.

The desired magnetization $\mathbf{m}_d(\omega_0)$ we use is specified by

$$\mathbf{m}_d(\omega_0) = \begin{cases} (m_x, m_y, m_z) = (0, 0, -1) \\ \quad \text{for } |\omega_0| > \text{SW}/2 - \delta\omega \\ (m_x, m_y, m_z) = (0, 0, +1) \\ \quad \text{for } |\omega_0| > \text{SW}/2 + \delta\omega \end{cases}. \qquad [10]$$

This is an ''ideal'' profile with an unspecified transition region of width $\pm\delta\omega$ left at the slice boundaries. As a rule of thumb, $\delta\omega \approx c_0$ could be tried as an initial guess with lower values used to sharpen the transition.

The mathematical programming optimization algorithm starts off with an initial pulse protrayed by its N sampling intervals $\{\Delta t_n\}$. The optimization program efficiently ''slides'' down the N-dimensional surface of the cost function until it sufficiently approaches a minimum.

A comment is due concerning the sign of the Δt_n variables. It is obvious that these variables must be nonnegative. This is not ensured, however, by the proposed algorithm which may yield negative Δt_n values. The situation is remedied by using the substitution $\Delta t_n = \beta_n^2$, yielding the cost function

$$J[\Delta t_1, \Delta t_2, \ldots, \Delta t_N] = J[\beta_1^2, \beta_2^2, \ldots, \beta_N^2].$$

The optimization is now performed with respect to the parameters $\{\beta_n\}$ which guarantees that the final sampling times are nonnegative.

The procedure is now demonstrated in two examples that represent the two extreme cases described above. The experimental setup was described in detail in (*16*), and the pulses were implemented on a Prestige 2T system (Elscint Ltd., Haifa, Israel)

The objective of our first example is to achieve a sharp transition which is typically useful when selective inversion of fat is required. Whereas the inverted bandwidth is less of an issue, our main concern is over the width of the transition. The pulse chosen for optimization was a 12 ms pulse which inverts a bandwidth of $\text{SW}/2\pi = 1$ kHz using maximal RF amplitude $x_f/2\pi = \gamma B_{1\,\max}/2\pi = 1$ kHz. The transition width parameter of the original pulse is chosen to be $c_0/2\pi = 120$ Hz. It is easily seen that the first term in Eq. [3] is much larger than the second so that our requirement is fulfilled. Moreover, as we expected, the equation yields a value of $\bar{\gamma}_0 = 4.1$. The dashed line in Fig. 1a depicts the computed response to this pulse. The optimization process is carried out in order to eliminate the large sidelobes which are clearly visible. It was performed over a frequency bandwidth of ± 1.5 kHz which was sampled at $K = 100$ points. The transition width of the desired magnetization was set to $2\delta\omega/2\pi = 100$ Hz. The cost functional weight factor of Eq. [9] was $\kappa = 2$. Figure 1 displays the results of the optimization, whereas Fig. 2 compares the transition of the optimized pulse with that of an equivalent sech/tanh pulse. The optimized pulse is seen to have a sharper transition and the sidelobes have indeed been eliminated.

The adiabatic behavior of the pulse is demonstrated by studying its sensitivity to inhomogeneity of the RF field. This is done by plotting contours of the longitudinal magnetization at the end of the pulse at each off-resonance frequency in the presence of field imperfections. In Fig. 3, these contours are plotted as a function of the maximal value of the applied RF field for the original and optimized pulses. The region enclosed by the dotted lines in Fig. 3b shows that the

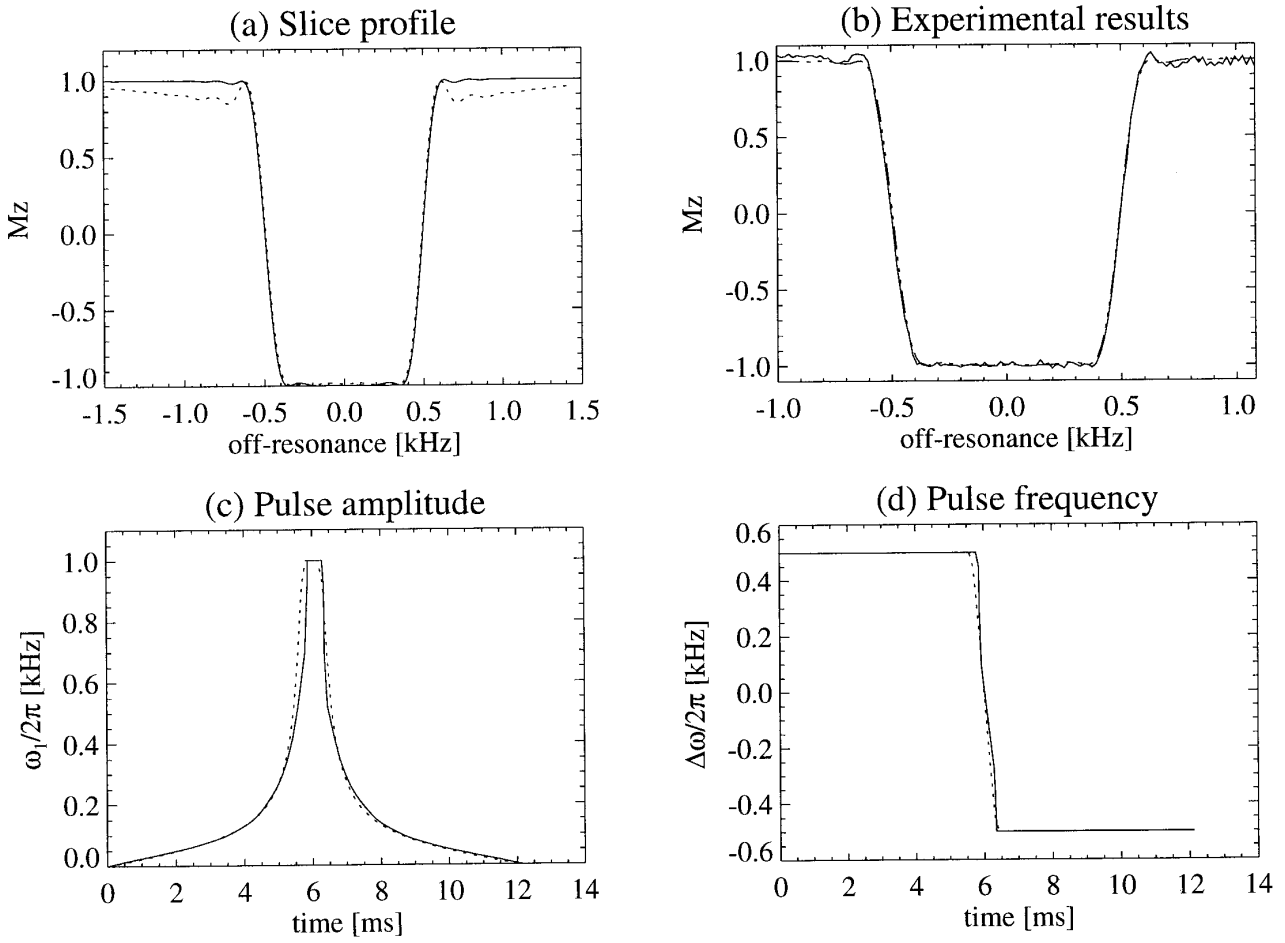

FIG. 1. Optimization of a pulse which is intended to achieve a sharp transition. (a) Slice profile, and pulse shape functions (c) amplitude and (d) frequency of original pulse (dotted line) and optimized pulse (solid line). (b) Experimental result (solid line) compared with simulated result (dashed line). Parameters of original pulse: duration, 12 ms; $(\gamma/2\pi)B_{1\,\max} = 1$ kHz; slice width, $\mathrm{SW}/2\pi = 1$ kHz. Transition width parameter, $c_0/2\pi = 120$ Hz. $\bar{\gamma}_0 = 4.1$.

optimized pulse retains a robust adiabatic behavior over a 100% variation in RF amplitude.

In our second example, an attempt is made to design a pulse which is capable of inverting a large bandwidth using a weak RF amplitude in a short time. This is achieved by sacrificing the transition width. We are trying to invert a bandwidth of $\mathrm{SW}/2\pi = 9$ kHz with an RF amplitude as low as $x_f/2\pi = \gamma B_{1\,\max}/2\pi = 1$ kHz. We attempt to use parameters that are more extreme than those discussed below Eq. [3]. In particular, we choose the transition width parameter $c_0/2\pi = 300$ Hz and the adiabatic parameter $\bar{\gamma}_0 = 2$ which yield a pulse of duration 5 ms. The resulting pulse exhibits a large ripple within the inverted band and a transition which levels off slowly (cf. the dashed line in Fig. 4a). It can be seen that now the second term in Eq. [3] dominates the first as required. The optimization was performed over a frequency bandwidth of ± 10 kHz which was sampled at $K = 100$ points. The transition width of the desired magnetization (Eq. [10]) was $2\delta\omega/2\pi = 800$ Hz. The cost-functional weight factor was $\kappa = 2$. The results are depicted in Fig. 4 which shows that only a small and tolerable ripple remains in the inverted magnetization and the sharpness of the transi-

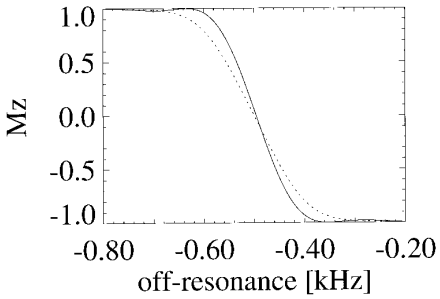

FIG. 2. Transition region of the optimized pulse of Fig. 1 (solid line) compared with that of an equivalent sech/tanh pulse (dotted line).

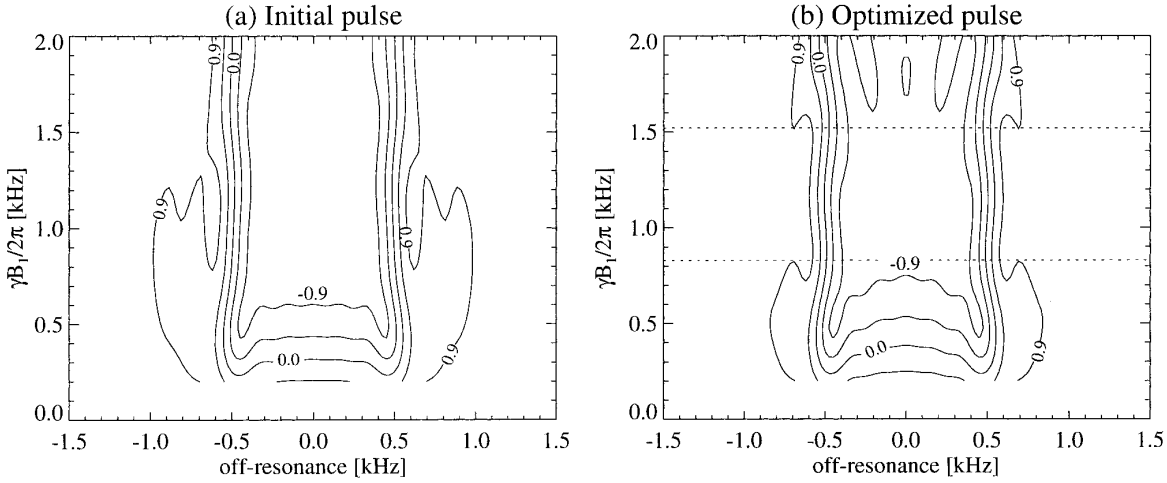

FIG. 3. Stability in the presence of RF field inhomogeneity: contours of the longitudinal magnetization at the end of the pulse at different RF amplitudes. (a) Original pulse and (b) Optimized pulse (corresponding to the pulse in Fig. 1).

tion is repaired. A sech/tanh adiabatic pulse with similar parameters is seen not to invert the magnetization (dotted line). The optimized pulse can also be shown to retain its stability over a 100% variation in RF amplitude.

In medical imaging applications, especially in high-field systems, the specific absorption rate (SAR) is an important specification of an RF pulse. The SAR measures the amount of RF energy dissipated by the patient's body per unit time.

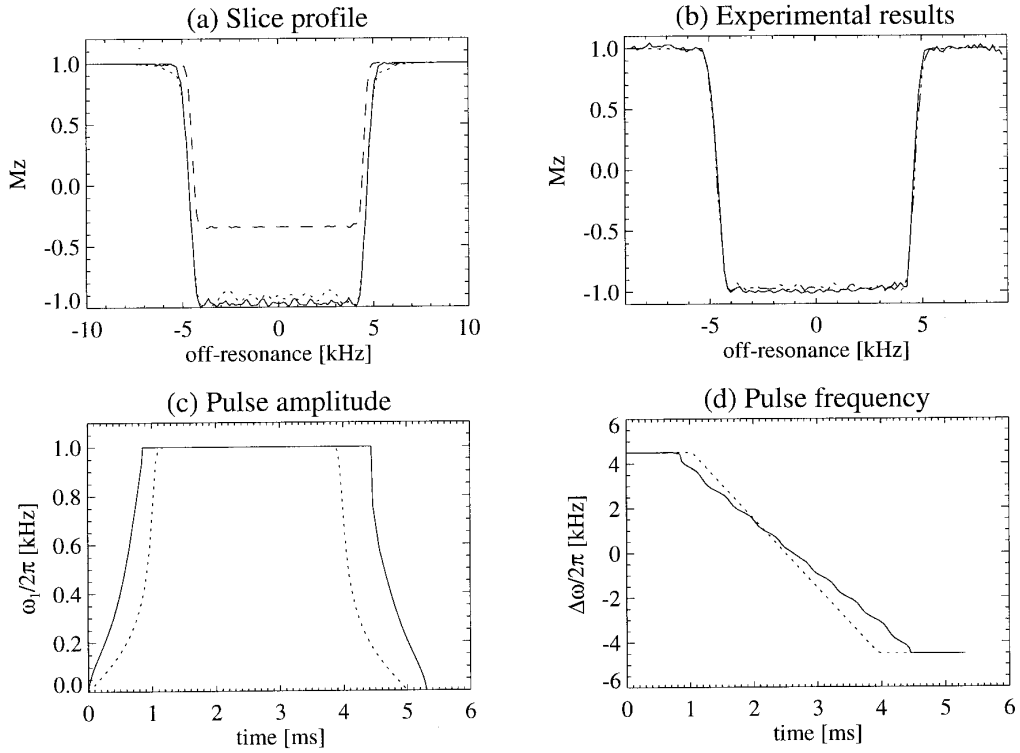

FIG. 4. Optimization of a pulse which is intended to invert a large bandwidth using a weak RF amplitude in a short time. (a) Slice profile, and pulse shape functions (c) amplitude and (d) frequency of original pulse (dotted line) and optimized pulse (solid line). (b) Experimental result (solid line) compared with simulated result (dashed line). Parameters of original pulse: duration, 5 ms; $(\gamma/2\pi)B_{1\,\max} = 1$ kHz; slice width, $\mathrm{SW}/2\pi = 9$ kHz. Transition width parameter, $c_0/2\pi = 300$ Hz. $\bar{\gamma}_0 = 2$. The slice profile is compared with a conventional sech/tanh adiabatic pulse with similar parameters (dashed line).

The RF energy of an RF pulse of duration T is proportional to

$$E_{\text{pulse}} \propto \int_{-T/2}^{T/2} (\gamma B_1(t))^2 dt.$$

The SAR induced by the pulse depends on the number of times per second that this pulse is employed. Comparing the energy of the optimized pulse with that of an equivalent sech/tanh pulse, both shown in Fig. 2, we obtain

$$\frac{E_{\text{example 1}}}{E_{\text{sech/tanh}}} = 0.4.$$

The two pulses have identical peak amplitude. The optimization has, therefore, achieved a large reduction in SAR level as well as a sharper transition. With regard to the second example, the situation is similar to that described in Ref. (*16*). Comparing the energy of the optimized pulse with the parameters shown in Fig. 4 ($\gamma B_{1\,\max}/2\pi = 1$ kHz) with a sech/tanh pulse of equal duration (a higher peak RF amplitude $\gamma B_{1\,\max}/2\pi = 1.8$ kHz must be used to achieve full inversion), we obtain

$$\frac{E_{\text{example 2}}}{E_{\text{sech/tanh}}} = 1.2.$$

In many practical applications, this slight increase in energy is unimportant as was discussed in Refs. (*16, 18*). Moreover, the peak RF amplitude is a critical restriction in practical MRI systems, and the optimized pulse performs the inversion using a significantly lower amplitude.

The adiabatic behavior of the outcome of the optimization is due to the trajectory constraint which was imposed on the optimization process; the effective field vector $\boldsymbol{\omega}_{\text{eff}}$ was confined to its original trajectory, in addition to which it was required to advance constantly along this path (i.e., backtracking was prohibited). Eliminating the trajectory constraint could induce abrupt motion of the effective field vector, thereby obstructing the adiabaticity (*17*).

It is important to reiterate that the flexible performance which we demonstrated is made possible by the tradeoff that our original pulse permits between the transition width $2c_0$ and the inverted frequency band SW; one may be sacrificed in favor of the other. This was illustrated in the examples by comparing our results with those of a conventional sech/tanh adiabatic pulse that does not allow such a tradeoff. Nevertheless, the optimization process brings about a deterioration in the adiabaticity of the pulse. In both our examples, it was verified that the pulses behave adiabatically over an approximately twofold range of variation in the RF field. This range ensures full inversion for coils that are used in high-field whole-body imaging (*19–21*).

Optimization using the trajectory constraint is not limited to the adiabatic pulse used in this paper. The same principle was successfully employed with respect to the sech/tanh adiabatic pulse (*22*). In this paper, we chose to demonstrate the procedure using our pulse since, to start with, it is more efficient than the sech/tanh pulse (*16*). Optimization methods which search for a local minimum are sensitive to the initial conditions used. It is, therefore, desirable to begin the process from the best possible pulse.

APPENDIX

Comparison of the New Adiabatic Pulse with the sech/tanh Pulse

In this Appendix, we quantitatively compare the performance of the conventional sech/tanh pulse with that of the adiabatic inversion pulse which was described in Ref. (*16*). The sech/tanh pulse (*4, 23*) is defined as follows in the frequency frame which rotates at the instantaneous frequency of the pulse

$$\omega_1(t) = x_f \operatorname{sech}(\beta t)$$
$$\omega(t) - \omega_c = \frac{\text{SW}}{2} \tanh(\beta t),$$

where x_f is the maximum RF amplitude, SW is the inverted bandwidth, and ω_c is the Larmor angular frequency at the slice center. The pulse duration T is associated with the parameter

$$\beta = 10.6/T \qquad [11]$$

so that the argument βt is given by $-5.3 \leqslant \beta t \leqslant 5.3$. The trajectory of this pulse is a half-ellipse (*23*). For convenience, we define the parameter

$$\upsilon = \frac{x_f}{\text{SW}/2},$$

which is the ratio between the two radii of the ellipse. Silver *et al.* (*24*) solved the Bloch equation analytically for the sech/tanh pulse. The final magnetization M_z at off-resonance $\Omega_0 = \omega_0 - \omega_c$ is given by

$$\frac{M_z(\Omega_0)}{M_0} = \tanh \pi\left(\frac{\Omega_0}{2\beta} + \frac{\mu}{2}\right) \tanh \pi\left(\frac{\Omega_0}{2\beta} - \frac{\mu}{2}\right) + \cos \pi\mu\sqrt{\upsilon^2 - 1} \operatorname{sech} \pi\left(\frac{\Omega_0}{2\beta} + \frac{\mu}{2}\right) \times \operatorname{sech} \pi\left(\frac{\Omega_0}{2\beta} - \frac{\mu}{2}\right), \qquad [12]$$

where M_0 is the equilibrium magnetization which is assumed to be in the z direction and μ is defined by

$$\mu = \frac{\mathrm{SW}/2}{\beta}. \qquad [13]$$

We will calculate (i) the transition width of the sech/tanh pulse and (ii) the minimal inversion time, T_m, which is the threshold duration required for the pulse to invert M_z.

Close to a transition, the first term in Eq. [12] is dominant over the second, leaving us with

$$\frac{M_z(\Omega_0)}{M_0} \simeq \tanh \pi\left(\frac{\Omega_0}{2\beta} + \frac{\mu}{2}\right)\tanh \pi\left(\frac{\Omega_0}{2\beta} - \frac{\mu}{2}\right). \qquad [14]$$

Each transition is then governed by one of the tanh functions so that the transition width is given by the frequency bandwidth needed for tanh α to switch between ± 0.95 with $\alpha = \pi(\Omega_0/(2\beta) + \mu/2)$, the argument. Therefore, $\alpha = \pm 1.83$. The transition width $\Delta\Omega_0 \equiv 2c_0$ is then given by

$$\pi \frac{\Delta\Omega_0}{2\beta} = 2 \times 1.83 \quad \Rightarrow \quad T \approx \frac{2}{c_0}, \qquad [15]$$

with c_0 given in frequency units (hertz). For the new adiabatic pulse, Eq. [4] yields

$$T \approx \frac{1.4}{c_0}, \qquad [16]$$

by substituting the minimal value of $\bar{\gamma}_0 \approx 4$. For a given pulse duration, the transition width of the new adiabatic pulse is sharper by a ratio of 1.4:2, as illustrated by Fig. 2.

The time T_{m} is the minimal pulse duration required to invert M_z at the Larmor frequency ω_{c} of the slice center (i.e., $\Omega_0 = 0$). We are interested in the case where we are trying to invert a large bandwidth with a low RF amplitude so that $v < 1$ is assumed. Moreover, we assume that half the transition region, given by Eq. [15] as $c_0 = 2/T$, must be smaller than half the slice width in frequency units

$$2\pi c_0 < \frac{\mathrm{SW}}{2} \quad \Rightarrow \quad \pi\mu > \frac{4\pi^2}{10.6} \approx 4, \qquad [17]$$

where SW is defined in angular frequency units and μ and β are defined by Eqs. [13] and [11]. From Eq. [12], we obtain for $\Omega_0 = 0$

$$\frac{M_z(\Omega_0 = 0)}{M_0} = -\tanh^2 \frac{\pi\mu}{2} + \cosh \pi\mu\sqrt{1 - v^2}\, \mathrm{sech}^2 \frac{\pi\mu}{2}. \qquad [18]$$

From Eq. [17], we can see that $e^{\pi\mu} \gg 1$ so that we can approximate

$$\tanh^2 \frac{\pi\mu}{2} \approx 1 - \frac{4}{e^{\pi\mu}}$$

$$\mathrm{sech}^2 \frac{\pi\mu}{2} \approx \frac{4}{e^{\pi\mu}}$$

$$1 + \cosh \pi\mu\sqrt{1 - v^2} \approx \frac{1}{2} e^{\pi\mu\sqrt{1-v^2}}.$$

If $v \ll 1$ so that $\sqrt{1 - v^2} \approx 1 - v^2/2$ and requiring an inversion of $M_z(\Omega_0)/M_0 = -0.98$, Eq. [18] yields

$$T_{\mathrm{m}} \approx 2.4 \frac{\mathrm{SW}}{x_f^2}, \qquad [19]$$

where SW and x_f are given now in frequency units. Equation [19] is obtained by using the definition [13] of μ. Equation [19] can be compared with the minimum inversion time of the new adiabatic pulse given in Eq. [5]. Substituting the minimal value of $\bar{\gamma}_0 \approx 4$, we obtain

$$T_{\mathrm{m}} \approx 0.64 \frac{\mathrm{SW}}{x_f^2} + \frac{2.14}{x_f}, \qquad [20]$$

where SW and x_f are in frequency units and the transition width is $c_0 = 0.522\, x_f$.

For $v < 1$, the new pulse, Eq. [20], performs much better than the sech/tanh pulse of Eq. [19]. For example, when a bandwidth of SW = 9 kHz is to be inverted using an RF amplitude of $x_f = 1$ kHz, the sech/tanh pulse would require 21.6 ms compared with 7.9 ms for the new pulse.

REFERENCES

1. K. Ugurbil, M. Garwood, A. R. Rath, and M. R. Bendall, *J. Magn. Reson.* **78,** 472 (1988).
2. C. P. Slichter, ''Principles of Magnetic Resonance,'' 3rd ed., Springer-Verlag, Berlin, 1992.
3. C. J. Hardy, W. A. Edelstein, and D. Vatis, *J. Magn. Reson.* **66,** 470 (1986).
4. M. S. Silver, R. I. Joseph, and D. I. Hoult, *J. Magn. Reson.* **59,** 347 (1984).
5. M. R. Bendall and D. T. Pegg, *J. Magn. Reson.* **67,** 376 (1986).
6. K. Ugurbil, M. Garwood, and A. R. Rath, *J. Magn. Reson.* **80,** 448 (1988).
7. G. Town and D. Rosenfeld, *J. Magn. Reson.* **89,** 170 (1990).
8. T. E. Skinner and P.-M. L. Robitaille, *J. Magn. Reson.* **98,** 14 (1992).
9. Ē. Kupče and R. Freeman, *J. Magn. Reson. A* **115,** 273 (1995).
10. Ē. Kupče and R. Freeman, *J. Magn. Reson. A* **117,** 246 (1995).
11. Ē. Kupče and R. Freeman, *J. Magn. Reson. A* **118,** 299 (1996).
12. A. Tannús and M. Garwood, *J. Magn. Reson. A* **120,** 133 (1996).

13. S. Conolly, D. Nishimura, and A. Macovski, *IEEE Trans. Med. Imaging* **MI-5,** 106 (1986).

14. S. Conolly, D. Nishimura, and A. Macovski, Abstracts of the Society of Magnetic Resonance in Medicine, 5th Annual Meeting, Montreal, Canada, p. 1456, 1986.

15. J. B. Murdoch, A. H. Lent, and M. R. Kritzer, *J. Magn. Reson.* **74,** 226 (1987).

16. D. Rosenfeld and Y. Zur, *Magn. Reson. Med.* **36,** 124 (1996).

17. D. Rosenfeld and Y. Zur, *Magn. Reson. Med.* **36,** 401 (1996).

18. D. Rosenfeld, S. L. Panfil, and Y. Zur, *Magn. Reson. Med.* **37,** 793 (1997).

19. G. H. Glover *et al., J. Magn. Reson.* **64,** 255 (1985).

20. P. S. Tofts, *J. Magn. Reson. B* **104,** 143 (1994).

21. T. K. F. Foo, C. E. Hayes, and Y. Kang, *Magn. Reson. Med.* **23,** 287 (1992).

22. D. Rosenfeld, S. L. Panfil, and Y. Zur, *in* ''Proceedings of the Society of Magnetic Resonance, 3rd Annual Meeting, and the European Society for Magnetic Resonance in Medicine and Biology, 12th Annual Meeting, Nice, France,'' p. 556, 1995.

23. S. Conolly, D. Nishimura, and A. Macovski, *J. Magn. Reson.* **83,** 549 (1989).

24. M. S. Silver, R. I. Joseph, and D. I. Hoult, *Phys. Rev. A* **31,** 2753 (1985).